Proceedings of ESDA2006
8th Biennial ASME Conference on Engineering Systems Design and Analysis
July 4-7, 2006, Torino, Italy

ESDA2006-95412

LOCALIZATION OF A MOBILE ROBOT WITH OMNIDIRECTIONAL WHEELS USING ANGULAR KALMAN FILTERING AND TRIANGULATION

Josep M. Font, Joaquim A. Batlle

Technical University of Catalonia (UPC)
Department of Mechanical Engineering
Avda. Diagonal 647, 08028 Barcelona, Catalonia, Spain
Tel. +34 93 405 4113, Fax +34 93 401 5813
E-mail: {josep.m.font, agullo.batlle}@upc.edu

ABSTRACT

Localization is one of the fundamental problems in mobile robot navigation. Several approaches to cope with the dynamic positioning problem have been made. Most of them use an extended Kalman filter (EKF) to estimate the robot pose –position and orientation– fusing both the robot odometry and external measurements.

In this paper, an EKF is used to estimate the angles, relative to the robot frame, of the straight lines from a rotating laser scanner to a set of landmarks. By using this method angles are predicted, between actual laser measurements, by means of the time integration of its time derivative, which depends upon the robot kinematics. Once these angles are estimated, triangulation can be consistently applied at any time to determine the robot pose. In this work, a mobile robot with three omnidirectional wheels –that consist of two spherical rollers– is considered. Computer simulations showing the accuracy of this method are presented.

INTRODUCTION

Mobile robots are increasingly used in flexible manufacturing industry and service environments. To achieve an autonomous operation, mobile robots must include a localization –or positioning– system in order to accurately estimate the robot pose –position and orientation– [1]. Nowadays, localization is one of the fundamental problems in mobile robot navigation.

In the last two decades, a number of different approaches have been proposed to solve the localization problem. These can be classified into two groups [2]: relative and absolute localization methods.

In relative localization, dead reckoning methods –odometry and inertial navigation– are used to calculate the robot position and orientation from a known initial pose. Odometry is a widely used localization method because of its low cost, high updating rate, and reasonable short path accuracy. However, its unbounded growth of time integration errors with the distance travelled by the robot is unavoidable and represents a significant inconvenience [3]. Several approaches have been done to cope with the odometry error propagation [4, 5].

Conversely, absolute localization methods estimate the robot position and orientation by detecting distinct features of a known environment. Most of the work published integrates a prediction phase, based on the odometric data and the robot kinematics, and a correction –or estimation– phase that takes into account external measurements. The most used methods are based on Kalman filtering [6-8] and Bayesian localization [9, 10]. Bayesian localization methods are robust to complex and badly mapped environments, but are in general less accurate. Finally, other authors deal with absolute localization using bounded-error state estimation applying interval analysis such in [11].

In this paper, an extended Kalman filter (EKF) is used to estimate in real time the angles –relative to the robot frame– of the straight lines from the sensor (a rotating laser scanner in this case) to a set of landmarks. Then, by means of triangulation, which refers to any process which solves a system of simultaneous algebraic or transcendental equations –whether or not they are reducible to an equivalent problem involving triangles– [12], the robot localization can be consistently determined at any time.

In mobile robotics, triangulation occurs often in the context of artificial landmarks. However, any natural aspects of the environment –such as walls or corners– whose positions are known, and are detected by a sensor whose indications depend on their position relative to the sensor, establish a triangulation context.

This approach is an extension of the method presented in [13], in which the odometry and laser sensor errors were not taken into account to predict the landmark angles for a tricycle type mobile robot with conventional wheels. In the work presented in [14], the sensor errors are considered and the use of a Kalman filter is proposed to predict the landmark angles for the same tricycle type industrial mobile robot.

In this paper, a mobile robot with three omnidirectional wheels equipped with a laser localization system is considered. Each omnidirectional wheel consists of two spherical rollers actuated by a single motor. The three motors allow the control of the three DOF of the robot plane movement.

The laser localization system consists of a rotating laser scanner and a set of catadioptric landmarks strategically placed. The scanner emits a laser beam that horizontally sweeps the environment and reflects back when it detects a landmark. Then, the angle of the reflected beam relative to the robot frame is measured.

In the following section, the triangulation methods for mobile robot localization and their properties are described. Next, the kinematics of the considered robot with omnidirectional wheels is presented and used to obtain the expressions for the angular state odometry. From these expressions, the dynamic angular state estimator is derived. Finally, computer simulations showing the positioning accuracy of the presented method –which is compared to other existing localization approaches– are reported.

TRIANGULATION BASED ROBOT LOCALIZATION

By means of triangulation it is possible to determine the robot position and orientation from the landmarks position and the measured angles θ_1, θ_2 and θ_3 –relative to the robot longitudinal axis– for three of them, Fig. 1 [15, 16]. As the accuracy of triangulation algorithms depends upon the point of observation and the landmark arrangements [15], more than three landmarks can also be used to improve the positioning accuracy [17, 18].

In this paper, a laser positioning system has been considered. The main advantage of this system is its high positioning accuracy inside the workspace which is required in certain practical situations. This system consists of a rotating laser scanner and a group of catadioptric landmarks strategically placed. The laser scanner emits a rotating beam that sweeps the environment and reflects back when it detects a landmark L_i. The system measures the angle θ_i of the reflected beam, relative to the vehicle longitudinal axis (Fig. 1), by means of an incremental encoder.

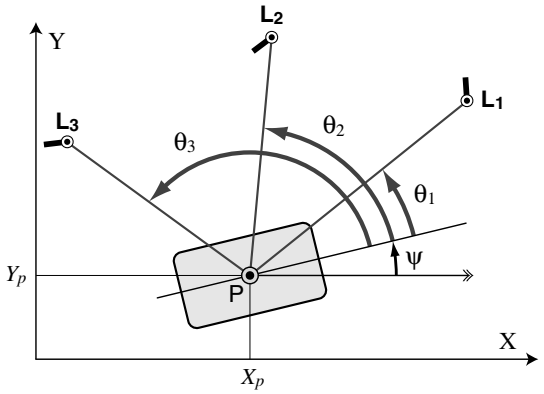

Fig. 1 The mobile robot pose can be calculated from landmarks position and angles θ_1, θ_2, θ_3 by triangulation

The consistent use of triangulation requires the relative angle to each landmark θ_i to be known at the same mobile robot pose, as it happens under static condition. However, this requirement is not fulfilled when robot moves because landmarks are detected at different poses of the robot, and therefore triangulation cannot be directly applied [19].

To solve this problem several authors use recursive algorithms to fuse the robot odometric information and the laser external measurements in order to keep track of the robot pose. In [7] a Kalman filtering framework is used to fuse this data. Other approaches are based on alternative recursive algorithms that deal with nongaussian noise and deterministic errors [20].

In this paper, to cope with dynamic positioning, an extended Kalman filter –which takes into account the errors associated to odometry and the laser scanner– is used to estimate the relative angles $\theta_i(t)$. Between actual laser measurements angles are predicted by means of the time integration of its time derivative, which depends upon the robot kinematics [13]. Thus, a kind of "angular odometry" substitutes the usual odometry related to the robot pose, and allows the kinematically consistent use of triangulation. The angular state vector used in the EKF is:

$$\boldsymbol{x}_k = \left\{\theta_{1,k}, \theta_{2,k}, ..., \theta_{N,k}\right\}^{\mathrm{T}}, \qquad (1)$$

instead of the conventional one $\boldsymbol{x}_k = \{x_k, y_k, \psi_k\}^{\mathrm{T}}$, which is obtained from the angular vector in Eq. (1) by means of triangulation. In Eq. (1), N represents the number of considered landmarks, in this case $N = 3$.

One of the advantages of the angular odometry developed is that, as it gives an accurate real-time estimation of each angle θ_i, it allows setting a narrow validation gate for each landmark reflection. Angular measurements that do not fall in this validation gate are ignored. If a reflection does not arrive inside the validation gate the angular odometric prediction continues over one more laser revolution. Therefore, the system is robust to possible outliers –wrong laser reflections– detected by the laser sensor.

ROBOT KINEMATICS

In this approach, a mobile robot with omnidirectional wheels, which consist of freely rotating spherical rollers, is considered. Figure 2 shows the real robot prototype SPHERIK-3x3. Each omnidirectional wheel is actuated by a single motor. The three motors allow the control of the three DOF of the robot plane movement. Figure 3 shows an omnidirectional wheel of the robot, with a free movement perpendicular to the actuated or motorized movement.

This wheel, developed by Batlle and Fortuny [21], guarantees the invariance of the jacobian matrix $\boldsymbol{J}$. This matrix relates the motor rotation velocities ω_j (j = 1, 2, 3) with the longitudinal and transversal components of the velocity of P –v_L and v_T respectively– and the robot angular velocity $\dot{\psi}$ (see Fig. 4):

$$\begin{Bmatrix}\omega_1\\ \omega_2\\ \omega_3\end{Bmatrix} = \boldsymbol{J}\begin{Bmatrix}v_L\\ v_T\\ \dot{\psi}\end{Bmatrix} = \frac{1}{r}\begin{bmatrix}0 & -1 & -L\\ \cos\alpha & \sin\alpha & -s\\ -\cos\alpha & \sin\alpha & -s\end{bmatrix}\begin{Bmatrix}v_L\\ v_T\\ \dot{\psi}\end{Bmatrix}, \qquad (2)$$

where r, L, s and α are geometric parameters defined in Fig. 4. The inverse of the jacobian matrix $\boldsymbol{J}^{-1}$ yields the following expression, in which velocities v_L, v_T and $\dot{\psi}$ are obtained from the motor rotation velocities ω_j:

$$\begin{Bmatrix}v_L\\ v_T\\ \dot{\psi}\end{Bmatrix} = \boldsymbol{J}^{-1}\begin{Bmatrix}\omega_1\\ \omega_2\\ \omega_3\end{Bmatrix} = \qquad . \quad (3)$$

$$= \frac{r}{s+L\sin\alpha}\begin{bmatrix}0 & \frac{s+L\sin\alpha}{2\cos\alpha} & -\frac{s+L\sin\alpha}{2\cos\alpha}\\ -s & \frac{L}{2} & \frac{L}{2}\\ -\sin\alpha & -\frac{1}{2} & -\frac{1}{2}\end{bmatrix}\begin{Bmatrix}\omega_1\\ \omega_2\\ \omega_3\end{Bmatrix}$$

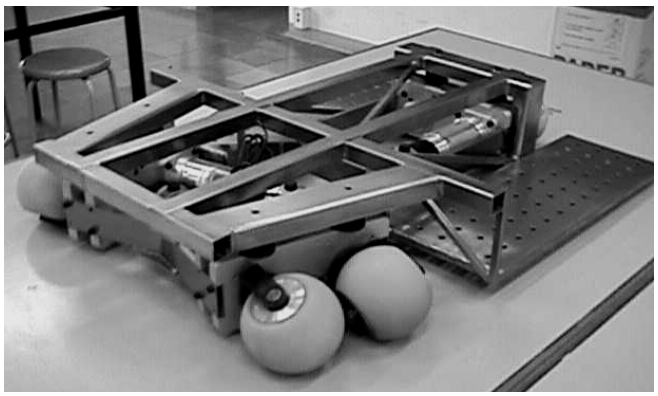

Fig. 2 Mobile robot SPHERIK-3x3

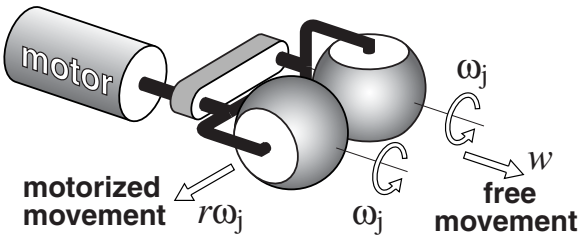

Fig. 3 Omnidirectional wheel that consists of two freely rotating spherical rollers

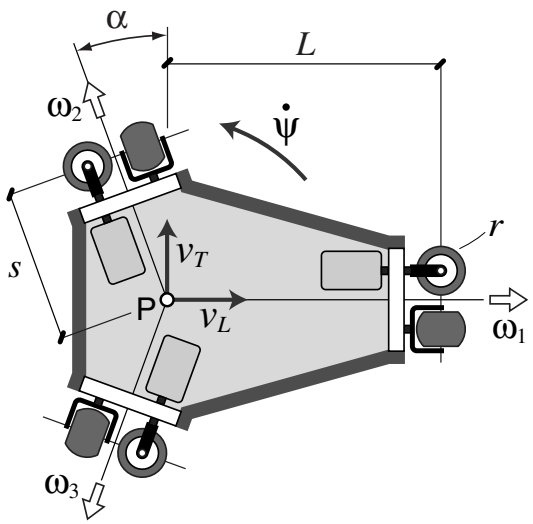

Fig. 4 Geometric and kinematical parameters of the mobile robot considered in Eq. (2)

It must be noted that an estimation of the kinematical variables v_L, v_T and $\dot{\psi}$ can be found at any time using Eq. (3), because the angular velocities ω_j are measured by the motor encoders.

As the SPHERIK-3x3 has the three degrees of freedom of the rigid body planar movement, it is a convenient platform to test different positioning techniques.

ANGULAR ODOMETRY

The solution presented to cope with triangulation under dynamic condition is based on the odometric calculation of the evolution of the angle –relative to the vehicle– of the straight lines from the laser scanner center to each landmark L_i. In the considered robot, point P (Fig. 4) is the center of the laser scanner.

If ρ_i stands for the distance between point P and the landmark L_i, and θ_i is the angle between the robot longitudinal axis and the straight line from P to this landmark (Fig. 5), the time evolution of θ_i can be expressed, according to the vehicle kinematics, as:

$$\dot{\theta}_i = \frac{\left(v_L \sin\theta_i - v_T \cos\theta_i\right)}{\rho_i} - \dot{\psi} \; . \qquad (4)$$

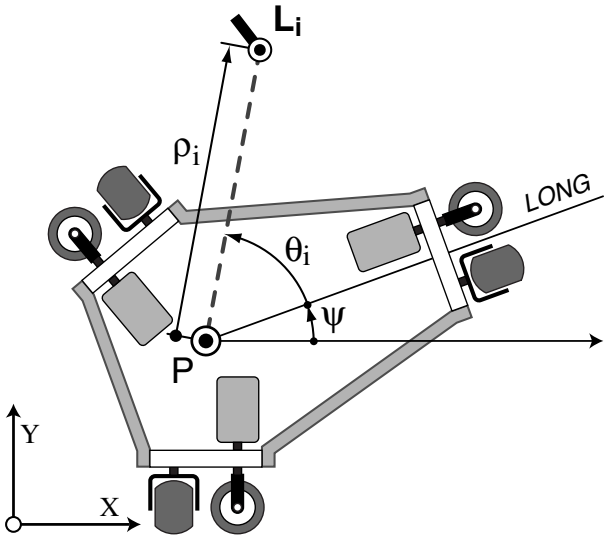

Fig. 5 Geometric variables ρ_i and θ_i associated with landmark L_i. P is the center of the laser scanner

Discrete time integration of Eq. (4) determines the evolution of angle θ_i between actual measurements:

$$\theta_{i,k} = f\left(\theta_{i,k-1}, \omega_{1,k-1}, \omega_{2,k-1}, \omega_{3,k-1}\right) = \\ = \theta_{i,k-1} + \left[\frac{\left(v_{L,k-1}\sin\theta_{i,k-1} - v_{T,k-1}\cos\theta_{i,k-1}\right)}{\rho_{i,k-1}} - \dot{\psi}_{k-1}\right]\Delta t \quad (5)$$

Variable ρ_i can be calculated once the angular state $\boldsymbol{x}_k$ has been estimated because it is the distance between P –the position of which is determined by angular triangulation– and the landmark L_i. Variables v_L, v_T and $\dot{\psi}$ are known from the odometric measurements ω_1, ω_2 and ω_3 using Eq. (3).

DYNAMIC ANGULAR STATE ESTIMATOR BASED ON KALMAN FILTERING

Kalman filtering is used to estimate at time step k the state vector $\boldsymbol{x}_k$ defined in Eq. (1), the dimension of which is the number N of landmarks considered. The nonlinear state transition function used in the EKF describes how the state $\boldsymbol{x}_k$ changes with time in response to a control input $\boldsymbol{u}_k$ and a noise disturbance $\boldsymbol{w}_k$:

$$\boldsymbol{x}_k = \boldsymbol{f}\left(\boldsymbol{x}_{k-1}, \boldsymbol{u}_{k-1}, \boldsymbol{w}_{k-1}\right). \quad (6)$$

The ith file (i = 1, ..., N) of this transition function $\boldsymbol{f}$, associated to the evolution of angle θ_i, is defined in Eq. (5). In the process considered, the control input vector $\boldsymbol{u}_k$ is calculated from the motor encoders at each time step k:

$$\boldsymbol{u}_k = \left\{\omega_{1,k}, \omega_{2,k}, \omega_{3,k}\right\}^{\mathrm{T}}. \quad (7)$$

Noise disturbances in the process model are associated to the measures of input variables ω_j (j = 1, 2, 3). These noises are assumed to be gaussian with zero mean and variance σ_ω^2, which has been experimentally determined. The measurement model of the EKF relates the state with the external measure $\boldsymbol{z}_k$ by means of the nonlinear observation function $\boldsymbol{h}$:

$$\boldsymbol{z}_k = \boldsymbol{h}\left(\boldsymbol{x}_k, \boldsymbol{v}_k\right), \quad (8)$$

where $\boldsymbol{v}_k$ denotes the measurement noise associated to the laser sensor, which also has been experimentally tested and assumed to be gaussian with variance σ_θ^2. Note that external measures $\boldsymbol{z}_k$ are directly the state of the filter. This fact simplifies the required calculations.

The goal of the state predictor is to produce an estimate of the angular state $\boldsymbol{x}_k$ at time k, based on the estimation $\boldsymbol{x}_{k-1}$ at time step k-1, the control input $\boldsymbol{u}_{k-1}$ and the landmark observation $\boldsymbol{z}_k$ (if any). The algorithm is composed by the following steps: prediction, observation, matching and estimation.

Prediction

The first step of the algorithm uses the state transition function –Eq. (6)– to predict the state at time k with the knowledge of $\boldsymbol{u}_{k-1}$:

$$\tilde{\boldsymbol{x}}_k = \boldsymbol{f}\left(\boldsymbol{x}_{k-1}, \boldsymbol{u}_{k-1}, 0\right). \quad (9)$$

Then, the state error covariance associated with this prediction is calculated:

$$\boldsymbol{P}_k^- = \boldsymbol{A}_k \boldsymbol{P}_{k-1} \boldsymbol{A}_k^{\mathrm{T}} + \boldsymbol{W}_k \boldsymbol{Q} \boldsymbol{W}_k^{\mathrm{T}}, \quad (10)$$

where $\boldsymbol{Q}$ is the covariance matrix associated with the noises $\boldsymbol{w}_k$ in the transition function $\boldsymbol{f}$, and matrices $\boldsymbol{A}_k$ and $\boldsymbol{W}_k$ are the jacobians defined by:

$$\boldsymbol{A}_k = \frac{\partial \boldsymbol{f}}{\partial \boldsymbol{x}}\left(\boldsymbol{x}_{k-1}, \boldsymbol{u}_{k-1}, 0\right), \quad (11)$$

$$\boldsymbol{W}_k = \frac{\partial \boldsymbol{f}}{\partial \boldsymbol{w}}\left(\boldsymbol{x}_{k-1}, \boldsymbol{u}_{k-1}, 0\right). \quad (12)$$

Observation and matching

In the following step, an angular measurement arrives and the innovation, which is the difference between the measured angle and the expected one, is calculated:

$$\boldsymbol{\upsilon}_{i,k} = \boldsymbol{z}_{i,k} - \boldsymbol{h}_i\left(\tilde{\boldsymbol{x}}_k, 0\right) = \theta_{i,k} - \tilde{\theta}_{i,k}. \quad (13)$$

The innovation covariance can be found by linearizing Eq. (8) around the prediction:

$$\boldsymbol{S}_k = \boldsymbol{H}_k \boldsymbol{P}_k^- \boldsymbol{H}_k^{\mathrm{T}} + \boldsymbol{V}_k \boldsymbol{R} \boldsymbol{V}_k^{\mathrm{T}}, \quad (14)$$

where $\boldsymbol{R}$ is the covariance matrix associated with the noise $\boldsymbol{v}_k$ in the laser measurements, and matrices $\boldsymbol{H}_k$ and $\boldsymbol{V}_k$ can be calculated by:

$$\boldsymbol{H}_k = \frac{\partial \boldsymbol{h}}{\partial \boldsymbol{x}}\left(\tilde{\boldsymbol{x}}_k, 0\right), \quad (15)$$

$$\boldsymbol{V}_k = \frac{\partial \boldsymbol{h}}{\partial \boldsymbol{v}}\left(\tilde{\boldsymbol{x}}_k, 0\right). \quad (16)$$

For each observation, a narrow validation gate is used to decide whether it is accepted or ignored:

$$\boldsymbol{\upsilon}_k^{\mathrm{T}} \boldsymbol{S}_k^{-1} \boldsymbol{\upsilon}_k \le g^2. \quad (17)$$

Therefore, the system is robust to outliers –erroneous laser reflections–. If a reflection does not arrive inside the validation gate, then the angular odometric prediction continues over one more laser revolution.

Estimation

In the last step, the successfully matched observations are used to update the angular state prediction. The Kalman filter gain $\boldsymbol{K}_k$ is calculated to compute the angular state estimation $\boldsymbol{x}_k$, and to update the covariance matrix $\boldsymbol{P}_k$:

$$\boldsymbol{K}_k = \boldsymbol{P}_k^- \boldsymbol{H}_k^{\mathrm{T}} \boldsymbol{S}_k^{-1}, \quad (18)$$

$$\boldsymbol{x}_k = \tilde{\boldsymbol{x}}_k + \boldsymbol{K}_k \boldsymbol{\upsilon}_k, \quad (19)$$

$$\boldsymbol{P}_k = \left(\boldsymbol{I} - \boldsymbol{K}_k \boldsymbol{H}_k\right) \boldsymbol{P}_k^-. \quad (20)$$

COMPARISON WITH THE POSE STATE EKF

In the presented approach to cope with the dynamic robot localization, an angular state EKF and triangulation are used to obtain an estimation of the robot pose at each time step. This method represents an alternative to the well-known pose state EKF [6, 7] in which positional odometry and the angular measurements are directly fused to get the optimal estimation of the robot pose. In this case, the EKF state vector is the robot pose –position and orientation– $\boldsymbol{x}_k = \{x_k, y_k, \psi_k\}^{\mathrm{T}}$, and the state transition function $\boldsymbol{f}$ is based on the positional odometry:

$$\boldsymbol{x}_k = \begin{Bmatrix} x_k \\ y_k \\ \psi_k \end{Bmatrix} = \begin{Bmatrix} x_{k-1} + \left(v_{L,k-1}\cos\psi_{k-1} - v_{T,k-1}\sin\psi_{k-1}\right)\Delta t \\ y_{k-1} + \left(v_{L,k-1}\sin\psi_{k-1} + v_{T,k-1}\cos\psi_{k-1}\right)\Delta t \\ \psi_{k-1} + \dot{\psi}_{k-1}\Delta t \end{Bmatrix}, \quad (21)$$

where variables v_L, v_T and $\dot{\psi}$ are known at time step k-1 from the odometric measurements ω_1, ω_2 and ω_3 using Eq. (3). The control input vector $\boldsymbol{u}_k$ is the same as in the angular state EKF –see Eq. (7)–, and the noise disturbances in the process model are also associated with the measures of input variables ω_j.

The measurement or observation function $\boldsymbol{h}$ of the pose state EKF approach relates the robot state –in this case the robot pose– with the angular measurement that arrives at time step k:

$$\boldsymbol{z}_{i,k} = \theta_{i,k} = \arctan\left(\frac{X_i - x_k}{Y_i - y_k}\right) - \psi_k, \quad (22)$$

where $\{X_i, Y_i\}$ is the position of landmark L_i. Once the nonlinear functions $\boldsymbol{f}$ and $\boldsymbol{h}$ are defined, the steps of the recursive EKF algorithm are the ones reported in the last section.

It must be noted that there are some differences between the presented angular state approach, and the conventional one based on the pose state EKF. One of the advantages of the presented method is related to the simplicity of the measurement equation, as the EKF state is directly measured. This fact simplifies the required calculations; for instance, matrix $\boldsymbol{H}_k$ is the identity at each time step k. Furthermore, the measurement equation is linear, and this implies a reduction of the linearization errors which are unavoidable in other equations.

A further difference is concerned with the use of the laser measurements to obtain the robot pose. In the pose state EKF, each angular measurement corrects the odometric pose estimation only in the degree of freedom perpendicular to the viewed landmark reflection. By means of the presented approach, once the angular state is estimated, the robot pose is globally determined using triangulation.

SIMULATION RESULTS

To illustrate the accuracy of the presented method, several computer simulations have been carried out. A realistic model of the robot motion and the sensors used has been created with *Simulink 6.1* (included in MATLAB R14). By means of this model it is possible to check different localization methods under the same environmental and sensor noise conditions.

Three 10 *m* straight trajectories with the same errors associated with the robot encoders and laser sensor measures, which have been experimentally modeled, have been simulated (trajectories 1, 2 and 3 in Fig. 6). Each trajectory is followed by the laser scanner center P at 1 ms^{-1} inside a 20 x 20 *m* environment with the landmark layout shown in Fig. 6. It must be remarked that during all the trajectories the robot orientation has remained constant and equal to 0 *rad*.

The laser scanner that has been simulated is a real instrument from *Guidance Control Systems Ltd* that rotates at 8 *Hz*. It delivers an accuracy of 0.1 *mrad*, and its maximum reflection distance is 30 *m*.

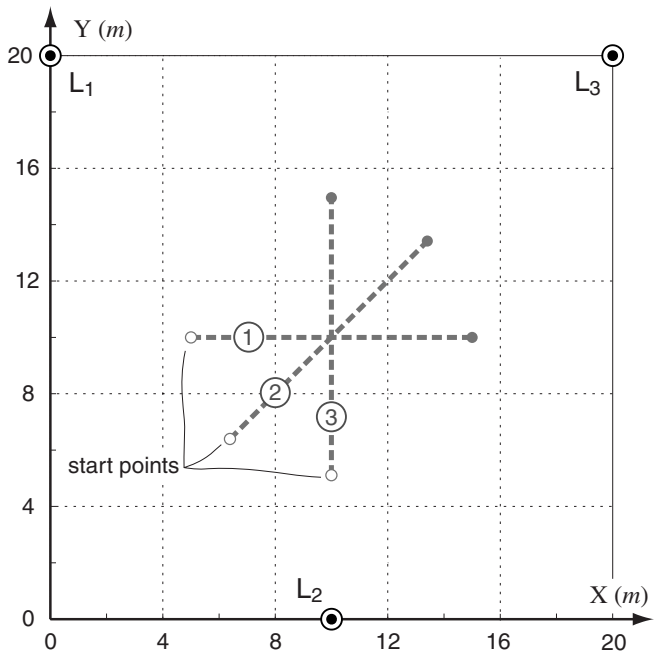

Fig. 6 Simulated robot trajectories and landmark layout in a 20 x 20 *m* environment

Tables 1, 2 and 3 show the statistical parameters of the lateral error between the actual robot trajectory and the calculated one when using three different approaches: The presented method –angular state EKF and triangulation–, the conventional extended Kalman filter to directly estimate the robot pose $\{x, y, \psi\}$ from laser measurements without triangulating [7], and the dynamic triangulation method previously presented in [13] –in which the sensor errors were not taken into account–.

Table 1 Comparison between the lateral error (e_{lat}) statistics using different methods (trajectory 1)

Localization method	RMSE e_{lat} [*mm*]	mean $\lvert e_{lat}\rvert$ [*mm*]	stand. dev. $\lvert e_{lat}\rvert$ [*mm*]
angular state EKF	0.51	0.41	0.30
pose state EKF	0.68	0.54	0.40
dynamic triangulation [13]	4.9	3.9	2.9

Table 2 Comparison between the lateral error (e_{lat}) statistics using different methods (trajectory 2)

Localization method	RMSE e_{lat} [*mm*]	mean $\lvert e_{lat}\rvert$ [*mm*]	stand. dev. $\lvert e_{lat}\rvert$ [*mm*]
angular state EKF	0.60	0.47	0.38
pose state EKF	2.2	2.0	0.85
dynamic triangulation [13]	3.5	2.8	2.1

Table 3 Comparison between the lateral error (e_{lat}) statistics using different methods (trajectory 3)

Localization method	RMSE e_{lat} [*mm*]	mean $\lvert e_{lat}\rvert$ [*mm*]	stand. dev. $\lvert e_{lat}\rvert$ [*mm*]
angular state EKF	0.53	0.43	0.31
pose state EKF	0.59	0.46	0.37
dynamic triangulation [13]	2.2	1.9	1.2

In Tables 1, 2 and 3 the first column indicates the root mean square error of the lateral error, while the others indicate the mean and the standard deviation of the lateral error absolute value respectively.

It can be noticed that, under the same conditions, the proposed method performs the best accuracy for the three trajectories. The dynamic triangulation algorithm yields the less accurate results because it does not take into account the sensor errors. Besides this, the standard deviation of the lateral error absolute value is also the lowest for the presented angular state EKF, which implies that its results are more reliable.

From the results obtained, it can be also observed that the accuracy of the presented method does not change significantly between different trajectories. Conversely, the error of the conventional pose state EKF grows significantly in trajectory 2 because each angular measurement corrects the odometric pose estimation only in the degree of freedom perpendicular to the viewed landmark reflection. This makes the pose state EKF algorithm more sensible to the landmark distribution around the trajectory. As a consequence, it can be concluded that the presented method is more appropriate for a general robot operation.

CONCLUSIONS

In this paper, a method to estimate the angles –relative to the robot longitudinal axis– of the straight lines from a laser sensor to a set of landmarks has been presented. This method uses an extended Kalman filter to estimate at each time an angular state vector by fusing the angular odometry –which depends on the robot kinematics– and the laser sensor angular measurements. By means of this discrete time estimator, triangulation can be consistently used at any time to determine the robot pose –position and orientation–.

The positioning accuracy of this method has been tested by means of computer simulations using *Simulink* (in MATLAB). For these simulations, a real 3-DOF mobile robot with omnidirectional wheels equipped with a laser positioning system has been considered. The presented approach has been compared to a previous method presented in [13] –in which the odometry and laser sensor errors were not taken into account– and to the conventional use of the EKF to directly estimate the robot pose without applying triangulation. In all the simulated trajectories, the presented angular state approach has turned out to be the best in terms of localization accuracy.

In the future, the method can be improved by using a parameter to evaluate in real time the accuracy of the positioning measurement. This parameter could help to optimise the simultaneous use of more than three landmarks.

Another future work will consist on the use of the real robot prototype SPHERIK-3x3 (Fig. 2), equipped with a laser positioning system, odometric sensors and the required hardware support, to validate the presented localization method. A precise system based on two incremental encoders and a linear potentiometer will be used to accurately measure the robot actual trajectory.

ACKNOWLEDGMENTS

This work has been partially supported by CeRTAP, Reference Center for Advanced Production Techniques of the Autonomous Government of Catalonia.

NOMENCLATURE

$\boldsymbol{A}_k$	Jacobian matrix of the partial derivatives of $\boldsymbol{f}$ with respect to $\boldsymbol{x}$
EKF	Extended Kalman filter
$\boldsymbol{f}$	EKF transition function
$\boldsymbol{H}_k$	Jacobian matrix of the partial derivatives of $\boldsymbol{h}$ with respect to $\boldsymbol{x}$
$\boldsymbol{h}$	EKF measurement or observation function
$\boldsymbol{J}$	Jacobian matrix for the kinematical control of the mobile robot
$\boldsymbol{K}_k$	Kalman filter gain
$\boldsymbol{P}_k$	State error covariance matrix
$\boldsymbol{Q}$	Process noise covariance
$\boldsymbol{R}$	Measurement noise covariance
$\boldsymbol{S}_k$	Innovation covariance matrix
$\boldsymbol{u}_k$	EKF control input vector
$\boldsymbol{V}_k$	Jacobian matrix of the partial derivatives of $\boldsymbol{h}$ with respect to $\boldsymbol{v}$
v_L, v_T	Longitudinal and transversal components of the velocity of the laser scanner center P
$\boldsymbol{v}_k$	Measurement noise
$\boldsymbol{W}_k$	Jacobian matrix of the partial derivatives of $\boldsymbol{f}$ with respect to $\boldsymbol{w}$
$\boldsymbol{w}_k$	Process noise
X_i, Y_i	Position of landmark L_i
$\boldsymbol{x}_k$	EKF state vector
x, y, ψ	Robot pose
$\boldsymbol{z}_k$	EKF external measurement vector
θ_i	Angle of the straight line from the laser scanner center to the landmark L_i relative to the robot longitudinal axis
ρ_i	Distance between the center of the laser scanner and the landmark L_i
σ_ω^2, σ_θ^2	Process noise variance and measurement noise variance
$\boldsymbol{\upsilon}_k$	EKF innovation
ω_1, ω_2, ω_3	Angular velocities of the robot motors
$\dot{\psi}$	Angular velocity of the robot

REFERENCES

[1] Leondes, C. T., 2000, *Mechatronic Systems Techniques and Applications Volume 2: Transportation and Vehicular Systems*, Gordon and Breach Science Publishers, Amsterdam.

[2] Borenstein, J., Everett, H. R., Feng, L., and Wehe, D., 1997, "Mobile Robot Positioning – Sensors and Techniques," Journal of Robotic Systems, Wiley Publishers, **14**(4), pp. 231-249.

[3] Kelly, A., 2004, "Linearized Error Propagation in Odometry," International Journal of Robotics Research, **23**(2), pp. 179-218.

[4] Wang, C. M., 1988, "Location Estimation and Uncertainty Analysis for Mobile Robots," *Proc. of the IEEE Int. Conference on Robotics and Automation*, Philadelphia, pp. 1230-1235.

[5] Borenstein, J., and Feng, L., 1995, "Correction of Systematic Odometry Error in Mobile Robotics," *Proc. of the IEEE Int. Conf. on Int. Robots and Systems*, Pittsburgh, pp. 569-564.

[6] Leonard, J. J., and Durrant-Whyte, H. F., 1991, "Mobile robot localization by tracking geometric beacons," IEEE Trans. on Robotics and Automation, **7**(3), pp. 376-382.

[7] Hu, H., and Gu, D., 2000, "Landmark-based navigation of autonomous robots in industry," International Journal of Industrial Robot, Emerald Group Publishing Limited, **27**(6), pp. 458-467.

[8] Welch, G., and Bishop, G., 2004, "An Introduction to the Kalman Filter," Technical Report TR 95-041, University of North Carolina at Chapel Hill.

[9] Burgard, W., Fox, D., Hennig, D., and Schmidt, T., 1996, "Estimating the Absolute Position of a Mobile Robot Using Position Probability Grids," *Proc. of the 14th National Conf. on Artificial Intelligence*, Portland, pp. 896-901.

[10] Dellaert, F., Fox, D., Burgard, W., and Thrun, S., 1999, "Monte Carlo Localization for Mobile Robots," *Proc. of the IEEE Int. Conf. Robotics and Automation*, Detroit, pp. 1322-1328.

[11] Kieffer, M., Jaulin, L., Walter, E., and Meizel, D., 2000, "Robust Autonomous Robot Localization Using Interval Analysis," Reliable Computing, Kluwer Academic Pub., **6**(3), pp. 337-362.

[12] Kelly, A., 2003, “Precision Dilution in Triangulation Based Mobile Robot Position Estimation,” *Proc. of the 8th Conference on Intelligent Autonomous Systems*, Amsterdam.

[13] Batlle, J. A., Font, J. M., and Escoda, J., 2004, “Dynamic Positioning of a Mobile Robot Using a Laser-based Goniometer,” *Proc. of the 5th IFAC/EURON Symposium on Intelligent Autonomous Vehicles*, Lisboa.

[14] Font, J. M., and Batlle, J. A., 2005, “Dynamic Triangulation for Mobile Robot Localization Using an Angular State Kalman Filter,” *Proc. of the 2nd European Conference on Mobile Robots*, Ancona, pp. 20-25.

[15] McGillem, C. D., and Rappaport, T. S., 1989, “A Beacon Navigation Method for Autonomous Vehicles,” IEEE Transactions on Vehicular Technology, **38**(3), pp. 132-139.

[16] Cohen, C., and Koss, F., 1993, “A Comprehensive Study of Three Object Triangulation,” *Proc. of the SPIE Conference on Mobile Robots*, Boston, pp. 95-106.

[17] Betke, M., and Gurvits, L., 1997, “Mobile Robot Localization Using Landmarks,” IEEE Transactions on Robotics and Automation, **13**(2), pp. 251-263.

[18] Madsen, C. B., and Andersen, C. S., 1998, “Optimal Landmark Selection for Triangulation of Robot Position,” Robotics and Autonomous Systems, Elsevier, **23**(4), pp. 277-292.

[19] Skewis, T., and Lumelsky, V., 1994, “Experiments With a Mobile Robot Operating in a Cluttered Unknown Environment,” Journal of Robotic Systems, Wiley Pub., **11**(9), pp. 281-300, 1994.

[20] Hanebeck, U. D., and Schmidt, G., 1996, “Set Theoretic Localization of Fast Mobile Robots Using an Angle Measurement Technique,” *Proc. of the IEEE Int. Conference on Robotics and Automation*, Minneapolis, pp. 1387-1394.

[21] Batlle, J. A., and Fortuny, G., 1998, “Omnidirectional wheel that consists of two spherical rollers for mobile robots,” *Proc. of the 13th National Conf. on Mechanical Engineering*, Terrassa, pp. 197-202 (in Spanish).